CrossMark

ORIGINAL PAPER

The dynamics of coupled populations subject to control

Stephanie J. Peacock[1] · Andrew W. Bateman[2,3,4] · Martin Krkošek[2,4] ·
Mark A. Lewis[1,3]

Abstract The dynamics of coupled populations have
mostly been studied in the context of metapopulation via-
bility with application to, for example, species at risk.
However, when considering pests and pathogens, eradica-
tion, not persistence, is often the end goal. Humans may
intervene to control nuisance populations, resulting in recip-
rocal interactions between the human and natural systems
that can lead to unexpected dynamics. The incidence of
these human-natural couplings has been increasing, hasten-
ing the need to better understand the emergent properties
of such systems in order to predict and manage outbreaks
of pests and pathogens. For example, the success of the
growing aquaculture industry depends on our ability to
manage pathogens and maintain a healthy environment for
farmed and wild fish. We developed a model for the dynam-
ics of connected populations subject to control, motivated
by sea louse parasites that can disperse among salmon
farms. The model includes exponential population growth
with a forced decline when populations reach a threshold,
representing control interventions. Coupling two popula-
tions with equal growth rates resulted in phase locking
or synchrony in their dynamics. Populations with different
growth rates had different periods of oscillation, leading
to quasiperiodic dynamics when coupled. Adding small
amounts of stochasticity destabilized quasiperiodic cycles
to chaos, while stochasticity was damped for periodic or
stable dynamics. Our analysis suggests that strict treatment
thresholds, although well intended, can complicate parasite
dynamics and hinder control efforts. Synchronizing pop-
ulations via coordinated management among farms leads
to more effective control that is required less frequently.
Our model is simple and generally applicable to other sys-
tems where dispersal affects the management of pests and
pathogens.

Keywords Aquaculture · Dispersal · Ecosystem service ·
Phase locking · Population dynamics · Synchrony

✉ Stephanie J. Peacock
  stephanie.peacock@ualberta.ca

[1] Biological Sciences, University of Alberta, Edmonton,
  Alberta T6G 2E9, Canada

[2] Ecology and Evolutionary Biology, University of Toronto,
  Toronto, Ontario M5S 3B2, Canada

[3] Mathematical and Statistical Sciences, University of Alberta,
  Edmonton, Alberta T6G 2G1, Canada

[4] Salmon Coast Field Station, Simoom Sound, British Columbia
  V0P 1S0, Canada

Introduction

As the global human population grows, there is an increas-
ing need to understand how interactions between human
and natural systems alter ecosystems and the services they
provide (Millennium Ecosystem Assessment 2005). Social
and ecological systems have traditionally been studied sep-
arately, but their integration as coupled human and natural
systems (CHANS) can reveal unexpected dynamics due to
nonlinearities and thresholds in the way that humans and
ecosystems interact (Liu et al. 2007). CHANS can exhibit
emergent properties, not present in isolated human or nat-
ural systems but resulting from the interactions between

them. There is a need to integrate studies of human actions with the natural dynamics of populations and communities to understand relevant feedbacks and develop effective policy that reduces human degradation of essential ecosystems services.

The natural dynamics of pests and pathogens have been of interest to scientists for some time, due to the economic importance of agricultural pests (Oerke 2006) and human cost of transmissible diseases (e.g., Keeling and Gilligan 2000). The role of dispersal among populations in hindering control efforts has long been recognized (e.g., Levins 1969). Theoretical models of coupled populations have shown that if neighboring populations fluctuate out of phase, such that high abundances at one location correspond to low abundances at another, dispersal can increase the probability of persistence via the rescue effect (Brown and Kodric-Brown 1977; Kendall and Fox 1998). The rescue effect is often thought of as beneficial in the context of population viability of endangered species, but in the context of disease, dispersal among local populations with asynchronous dynamics may hinder efforts to eradicate disease (e.g., Bolker and Grenfell 1996). Mathematical models (e.g., Liebhold et al. 2004; Holt and McPeek 1996; Hastings 1993) and observational data (e.g., Ranta et al. 1995; Steen et al. 1996) have suggested that dispersal will tend to synchronize local populations. Synchronized populations are more susceptible to extinction because stochastic events or human intervention can cause catastrophic losses when all populations are at low abundance, with little opportunity for recolonization. Paradoxically, dispersal could therefore help or hinder efforts to control disease in metapopulations depending on whether dispersal results in synchronized pathogen dynamics, or the rescue effect (Abbott 2011).

Treatments with chemotherapeutants and wildlife culls (e.g., to reduce disease transmission) are examples of control efforts that result in an immediate decline in the unwanted populations, but resurgence may be swift if nearby populations persist. The optimal allocation of control effort among subpopulations may depend on the level of connectivity and relative growth rates of the populations. For example, in control of the yellow legged herring gull, a nuisance species in the western Mediterranean, the magnitude of the cull and life stage to be targeted depends on the dispersal rate (and relative growth rates) among gull populations (Brooks and Lebreton 2001). Tuberculosis in New Zealand possums can be controlled by culling infected individuals with poison baits, but the effectiveness of this control depends on the timing of application and spatial configuration of habitat patches (Fulford et al. 2002). In general, asynchrony in the dynamics of disease among host local populations likely decreases the probability of successful eradication (Earn et al. 1998). Indeed, it has been proposed that efforts to eradicate measles on a global

scale were hampered after vaccination programs of the late 1960s inadvertently resulted in the decorrelation of measles epidemics in UK cities (Bolker and Grenfell 1996).

The motivation for this study came from parasite dynamics in open-net aquaculture; a coupled human and natural system where the eradication of pathogens has proved difficult. The rapid expansion of aquaculture (FAO 2014) has resulted in changes to coastal ecosystems including the emergence of disease (Walker and Winton 2010) and transmission of pathogens between farmed and wild fish (Heggberget et al. 1993). In regions where farmed and wild fish coexist, the health of the system depends on effective management of disease in farmed fish (Peacock et al. 2013; Tompkins et al. 2015). Connectivity among populations in the marine environment is typically higher than in terrestrial systems (McCallum et al. 2003), and dispersal of pathogens among host populations can complicate disease control.

In particular, parasitic copepods known as sea lice or salmon lice, predominantly *Lepeophtheirus salmonis* and *Caligus* spp., have been a persistent problem in salmon aquaculture, costing millions of dollars in treatment and reduced feed conversion ratios, negatively impacting fish health, and damaging public perception of farmed salmon (Costello 2009). Many approaches have been taken to minimize sea louse outbreaks, including biomass restrictions to limit host density, strategic siting of farms, the use of cleaner fish that prey on sea lice, and the application of chemotherapeutants (Rae 2002; Brooks 2009). Sea louse populations on salmon farms within a region are connected via the dispersal of free-living larvae (Adams et al. 2012), and studies have shown that critical host density thresholds for sea lice exist at regional scales (Frazer et al. 2012; Jansen et al. 2012; Kristoffersen et al. 2013). It has been estimated that 28 % of infections are due to the influx of larvae from neighboring farms (Aldrin et al. 2013). This connectivity among farms affects the growth of sea louse populations on any given farm and the efficacy of treatments. Furthermore, frequent and less effective use of chemotherapeutants may facilitate the evolution of resistance in sea lice (Aaen et al. 2015), which is a major challenge facing the aquaculture industry (Igboeli et al. 2014). Coordination of management among farms may be a key in effectively managing sea lice (Kristoffersen et al. 2013), as well as the spread of other pathogens. Many studies have focused on statistical analyses of monitoring data to uncover the relationships among farms (e.g., Jansen et al. 2012; Aldrin et al. 2013; Rogers et al. 2013; Revie et al. 2002) but much can be learned from applying more general theoretical models of population and disease dynamics (e.g., Frazer et al. 2012).

In this paper, we develop a simple model for the dynamics of two populations connected by dispersal, where each population is subject to external control when it reaches a threshold density. The model complements previous work

examining sea louse populations on individual salmon farms (Krkošek et al. 2010; Rogers et al. 2013) and within a region (Jansen et al. 2012; Aldrin et al. 2013) to explicitly examine how connectivity between parasite populations on adacent farms can alter the timing and frequency of treatments. This work also builds on our general theoretical understanding of how dispersal (Hastings 1993; Goldwyn and Hastings 2011; Dey et al. 2015; Kendall and Fox 1998) and intervention (Chau 2000; Sah et al. 2013) affect the dynamics of coupled populations. The model was motivated by sea lice on farmed salmon but has general applicability to other systems where dispersal affects control, such as in agricultural pests of crops within a region (Ives and Settle 1997), and transmissible diseases in wildlife (Tompkins et al. 2015) and humans (e.g., Bolker and Grenfell 1996).

Methods

A simple model for growth and control

Analyses of sea louse population dynamics on isolated salmon farms suggest that parasite populations grow exponentially in the absence of treatment (Krkošek et al. 2010; Rogers et al. 2013). Exponential growth is not unique to sea lice and has been observed in birds (Van Bael and Pruett-Jones 1996), mammals (Silva 2003), and insects (Birch 1948) and has been used to describe dynamics of other agricultural pests (e.g., Samways 1979). Although negative density dependence will regulate populations at some point, management intervention in the case of pests and parasites may prevent populations from reaching such high densities. Thus, although the following model was motivated by sea louse parasites on salmon farms, it likely has broad applicability and may inform management of other pests and parasites. In developing the model, we refer to populations in adjacent patches rather than parasites on adjacent salmon farms to maintain this generality.

The dynamics of two populations that are continuously coupled by dispersal are described by

$$\begin{bmatrix} u \\ v \end{bmatrix}' = \begin{bmatrix} r_{uu} & r_{uv} \\ r_{vu} & r_{vv} \end{bmatrix} \begin{bmatrix} u \\ v \end{bmatrix}, \tag{1}$$

where u is the population density in patch one, v is the population density in patch two, r_{ii} is the internal growth rate of population i where $i = u$ or v and r_{ij} is the connectivity probability from population j to population i. We refer to the total growth rate of population $i = u$ or v as the row sum of internal growth and connectivity: $r_{ii} + r_{ij}$. The solutions for $u(t) = f_u(t, u_0, v_0)$ and $v(t) = f_v(t, u_0, v_0)$ are given in Appendix A.

We included control treatments by forcing a reduction in a population when it reached the threshold abundance

of N_{max}. Many countries, including Norway, Ireland, the USA, and Canada, require salmon farms to treat their fish with chemotherapeutants when a threshold sea louse abundance is reached, but this threshold may vary among regions (Brooks 2009). For our simulations, we chose $N_{max} = 3$ motile lice per fish, based on guidelines in Pacific Canada that recommend treatment when farmed salmon have an average of three lice per fish (British Columbia Ministry of Agriculture and Lands 2005), but the value of the threshold is arbitrary for the qualitative analysis we perform here. Observations suggest that chemotherapeutants may kill up to 95 % of motile sea lice on treated farmed salmon (Lees et al. 2008), although treatment efficacy may be lower in many regions and is undoubtedly changing (Aaen et al. 2015). We assumed that treatments were effective, and when either $u(t)$ or $v(t)$ exceeded N_{max}, we modeled a treatment of that population by forcing the dynamics to reset with the initial condition for the treated population being a 95 % reduction from the threshold (i.e., $N_{min} = (1 - 0.95)N_{max}$) and the initial condition for the untreated population being equal to the density prior to treatment of the other population. For example, starting with initial population densities u_k and v_k at $t = 0$, if $u(t)$ reaches the threshold N_{max} at time $t = T_u$, the system would be reset with $t = 0$ and initial conditions $u_{k+1} = N_{min}$ and $v_{k+1} = f_v(T_u, u_k, v_k)$. The subscript k here represents the treatment number counted across both populations. In the following section, we develop a discrete-time model that describes the population density at treatment $k+1$ based on the population density at treatment k.

Discrete-time treatment dynamics

We aimed to understand the conditions under which the populations will become synchronized, settle into a regular pattern of alternating treatments, or have unpredictable treatment timing. To this end, we reduced the dimensionality of the system while retaining key properties (Schaffer 1985) by deriving a discrete-time map for the population density in a focal population when the other population is treated. This approach is related to "peak to peak" dynamics of time series data in which past maxima are used to predict future peaks in time series oscillations (e.g., Rinaldi et al 2001). A similar approach is also often used to reduce the dimensionality of a system of three or more differential equations by plotting successive points where the three-dimensional phase dynamics pass through a two-dimensional plane, called a Poincaré section (e.g., Hastings and Powell 1991; Schaffer 1985).

Given the initial population densities in the two patches, we solved Eq. 1 for the time, T_u, until population u reaches the treatment threshold (Appendix A) and the time, T_v, until population v reaches the treatment threshold. We calculated

$\widetilde{T} = T_u - T_v$, where $\widetilde{T} < 0$ indicates that the treatment of u will happen next, and $\widetilde{T} > 0$ indicates that the treatment of v will happen next. The population densities after the next treatment $k + 1$ are therefore

$$\begin{bmatrix} u \\ v \end{bmatrix}_{k+1} = \underbrace{\left(1 - H(\widetilde{T})\right) \begin{bmatrix} N_{\min} \\ f_v\left(T_u, u_k, v_k\right) \end{bmatrix}}_{u \text{ is treated}} + \underbrace{H(\widetilde{T}) \begin{bmatrix} f_u\left(T_v, u_k, v_k\right) \\ N_{\min} \end{bmatrix}}_{v \text{ is treated}}, \quad (2)$$

where $H(\widetilde{T})$ is the Heaviside step function that equals zero when $\widetilde{T} < 0$ and one otherwise. We used the dynamical system described by Eq. 2 to construct a return map that takes the u when v is initially treated, u^*, and returns u the next time v is treated, $\phi(u^*)$. We refer to $\phi(u^*)$ as the population density (in patch one) at re-treatment (of patch two). We show in Appendix B that the general equation for this return map is

$$\phi(u^*) = \underbrace{H(\widetilde{T}_0) \, f_u\left(T_{v0}, u^*, N_{\min}\right)}_{m=0} + \underbrace{\left[\sum_{m=1}^{\infty} H(\widetilde{T}_m) \prod_{n=0}^{m-1} [1 - H(\widetilde{T}_n)]\right] f_u\left(T_{vm}, N_{\min}, v_{m-1}\right)}_{m \geq 1},$$

(3)

where treatment of u occurs m times before v is treated again. The time between treatment $m - 1$ and the next treatment of v is denoted T_{vm}, and $\widetilde{T}_m = T_{um} - T_{vm}$. The value of m depends on the relative growth rates of the two populations and the magnitude of connectivity. The values of T_{um} and T_{vm} cannot be solved for explicitly (Appendix A); therefore, we simulated the dynamics using a recursive algorithm to obtain the shape of $\phi(u^*)$ (Appendix C).

Parameter sensitivity

We investigated the dynamics of the return map for a limited number of parameter combinations with each growth rate constrained between zero and two. A comprehensive description of the dynamics of the return map under all parameter combinations was impossible because the return map had to be simulated, so we focused on results from four scenarios that describe parameter changes that might occur in networks of salmon farms (Table 1). First, we considered a scenario where the internal growth rates were constant and equal at $r_{uu} = r_{vv} = 1.00$ and connectivity increased from 0.01 to 1.00 in increments of 0.01 ($r_{uv} = r_{vu} = r_{ij}$, scenario

Table 1 Summary of scenarios for how increasing connectivity affects dynamics

Scenario	Growth rates			
	u internal	v internal	from u to v	from v to u
	r_{uu}	r_{vv}	r_{vu}	r_{uv}
A	1.00	1.00	$0.01 \to 1.00$[a]	$0.01 \to 1.00$[a]
B	1.00	1.00	$0.01 \to 1.00$	0.01
C	1.00	0.50	$0.01 \to 1.00$	$0.01 \to 1.00$
D	1.00	0.50	$0.01 \to 1.00$	0.01

[a] Under scenario A, we considered connectivity increasing to 2.00 when assessing the frequency of treatments.

A). This scenario could represent two salmon farms being brought closer together, increasing exchange of parasites between them. Second, we considered increasing r_{vu} from 0.01 to 1.00 but connectivity in the other direction constant at $r_{uv} = 0.01$ (scenario B). This scenario could represent an increase in the advection of larvae from one farm to another. The third scenario had connectivity equal and increasing as in scenario A, but u had twice the internal growth rate as v ($r_{uu} = 1.00, r_{vv} = 0.50$, scenario C). Similarly, in scenario D, u had twice the internal growth rate as v, but r_{vu} increasing from 0.01 to 1.00. Different internal growth rates could represent different host population sizes or environmental conditions affecting growth on the two farms.

In each scenario, for each value of the appropriate control parameters (i.e., r_{vu}, and r_{uv} in scenarios A and C; Table 1), we simulated the return map over 2000 iterations starting at $u_0^* = 2.7$. We constructed a bifurcation diagram by plotting the values of $\phi(u^*)$ for the last 500 iterations, over the value of the control parameter. We present the results for $u_0^* = 2.7$, but we examined the bifurcation diagrams starting from several values of u_0^* to check that the long-term dynamics were not dependent on the initial conditions (Online Resource, Fig. S1).

We also considered the long-term frequency of treatments over increasing connectivity between populations. To calculate the frequency of treatments, we first iterated the return map 500 times starting at $u^* = 2.7$ to remove transient dynamics and then simulated the dynamical system given by Eq. 2 for 100 treatments, where treatments were counted across both populations. If the two populations were treated at the same time, we considered it two treatments. The frequency of treatments was then calculated as 100 divided by the time taken to reach 100 treatments. To examine how connectivity affects the frequency of treatments independent of overall increases in the growth rates, we also considered a variation on scenario A in which the internal growth rate declined as connectivity increased such

that $r_{ii} = 1 - r_{ij}$ and the total growth rates to populations remained constant (Online Resource).

Testing for chaos

Under certain parameter values, the numerically calculated return map given by Eq. 3 had a discontinuity at the point where u was treated m times or $m + 1$ times, depending on the population density u^* at the first treatment of v (see "Results"). This discontinuity resulted in cyclic behavior that was difficult to classify by numerical simulations as periodic or chaotic (Galvanetto 2000). Chaos is extreme sensitivity to initial conditions and can be classified by calculating the rate of divergence between two trajectories that are initially close (Hastings et al. 1993). This rate is known as the Lyapunov exponent λ where $\epsilon_n = \epsilon_0\, e^{\lambda n}$, $\epsilon_0 << 1$, and ϵ_n is the difference between a perturbed and fiducial trajectory after n iterations of the return map. Positive exponents indicate that two trajectories will diverge, and therefore, the dynamics are sensitive to the initial condition, characteristic of chaos (Sprott 2003; Hastings et al. 1993).

To determine if the return map lead to chaotic dynamics under the scenarios we considered, we numerically calculated the Lyapunov exponent for all parameter combinations (Table 1) as

$$\lambda = \sum_{n=1}^{10^4} \log\left(\frac{|\epsilon_n|}{\epsilon_0}\right). \qquad (4)$$

For discontinuous return maps such as ours, Eq. 4 is not valid if the fiducial and perturbed trajectories project onto different pieces of the return map (Galvanetto 2000). To avoid this problem, we chose a small initial difference between the trajectories of $\epsilon_0 = 10^{-8}$. At each iteration of the return map, we readjusted the two trajectories bringing them back together along the line of separation such that the difference between them was ϵ_0, with the sign of the difference equal to the sign of ϵ_{n-1} (Sprott 2003, p. 116–117):

$$\epsilon_n = \phi\left(\phi^{n-1}(u^*) + \frac{\epsilon_{n-1}}{|\epsilon_{n-1}|}\epsilon_0\right) - \phi^n(u^*) \qquad (5)$$

where $\phi^n(u^*)$ represents the nth iteration of the fiducial trajectory (i.e., $\phi^2(u^*) = \phi(\phi(u^*))$). This correction made it very unlikely that the two trajectories would project onto different pieces of the return map, as the difference between them remained relatively small. In all our simulations, we verified that $\epsilon_n << 1$, suggesting that the two trajectories had projected on to the pieces of the return map.

In the numerical calculation, the value of the Lyapunov exponent may depend on the choice of u_0^* (Earnshaw 1993), so we repeated the calculation of Eq. 4 for three randomly-chosen values between N_{min} and N_{max}. For each starting value, we iterated the map 200 times to remove transient

dynamics and then used the subsequent 10 000 iterations in the calculation of λ (Sprott 2003). We report the mean value of λ over the three values of u_0^* for each value of connectivity described in Section "Parameter sensitivity."

Stochasticity

Environmental stochasticity may influence the growth of populations, as is the case for sea louse populations on salmon farms (Aldrin et al. 2013; Rogers et al. 2013). We added stochasticity to the return map and evaluated its influence on the long-term dynamics. At each iteration, we multiplied $\phi(u^*)$ by a log-normal distribution with mean one and standard deviation on the log scale of $s = 10^{-2}$ (Hilborn and Mangel 1997). We compared the stochastic dynamics for parameters that corresponded to a quasiperiodic cycle with a Lyapunov exponent close to zero in the deterministic model versus those that produced periodic dynamics or had a single equilibrium with a Lyapunov exponent that was relatively large and negative in the deterministic model. We examined 200 iterations of the return map for two trajectories: one fiducial trajectory starting at $u_0^* = 2.7$ and a second perturbed trajectory initially separated by a small distance $\epsilon_0 = 10^{-8}$ from the fiducial trajectory. We compared the difference between these trajectories over increasing iterations and also calculated the Lyapunov exponent, with and without stochasticity in the model. In calculating the Lyapunov exponent for the stochastic return map, we used an independent sequence of log-normal values for the fiducial and perturbed trajectories. To ensure the value of λ in the stochastic model was not sensitive to the particular log-normal random values in the simulation, we repeated the calculation 50 times and report the mean and range.

Results

Simulations of simple model

Simulations of the model predicted that for two isolated populations (i.e., $r_{ij} = 0 \ \forall \ i \neq j$), each population will oscillate with treatments occurring at regular intervals. The frequency of treatments was dictated by the internal population growth rate r_{ii}, with higher growth rates resulting in more rapid resurgence of the population after treatment and therefore a higher frequency of treatments.

When we coupled the two populations, the dynamics were more complex. Simulations displayed a range of behavior including alternating treatments (i.e., phase locking; Fig. 1a), synchrony between the populations (Fig. 1b), or seemingly chaotic dynamics (Fig. 1c; Table 2). To better understand this complex behavior, we considered a
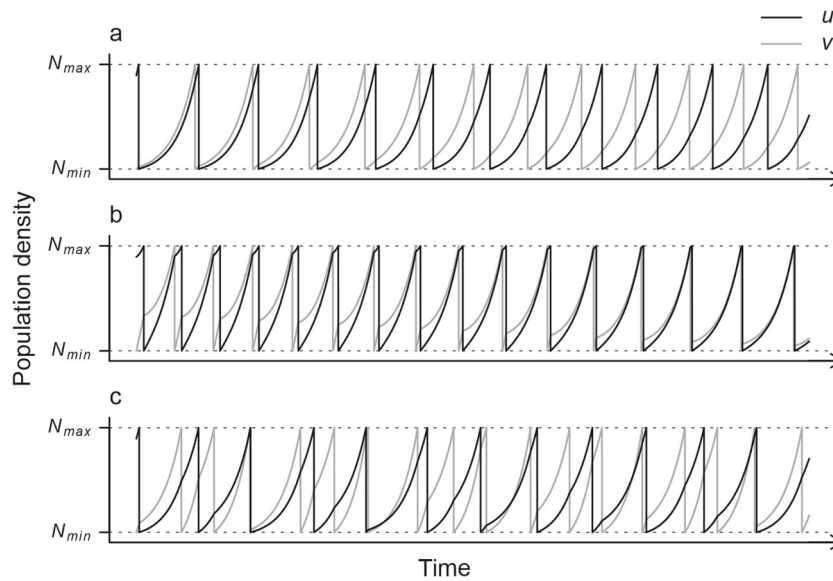
Fig. 1 Three types of behavior observed were observed for connected populations subject to control: **a** alternating treatments of populations for equal growth rates of the two populations and connectivity less than the internal growth rates ($r_{ij}/r_{ii} = 0.1$), **b** synchrony in the population dynamics between patches for equal growth rates of the two populations and connectivity greater than the internal growth rates ($r_{ij}/r_{ii} = 10$), and **c** apparently chaotic dynamics where the treatment timing was unpredictable for unequal growth rates of the two populations. Initial conditions were $u_0 = 2.7$ (*black line*) and $v_0 = N_{\min}$ (*gray line*). The *upper and lower horizontal dashed lines* indicate the treatment threshold and abundance of parasite immediately after treatment, respectively

one-dimensional discrete-time return map describing the change in u in between treatments of v.

Discrete-time treatment dynamics

For two populations that have identical growth rates but low connectivity, the return map had a stable equilibrium in the open interval ($N_{\min}, N_{\max}$) (the exact value depended on the level of connectivity) and unstable equilibria at $N_{\min}$ and at $N_{\max}$. This dynamical behavior is termed phase locking because the two populations had the same period but their dynamics were shifted out of phase by a fixed amount (Becks and Arndt 2013). The consequence was alternating treatments of u and v, with a stable equilibrium for the population density u whenever v was treated (Figs. 1a and 2a). If both populations were treated at the same time, u was exactly at the unstable equilibrium. In this case, the two populations remained synchronized because the period of their oscillations was identical.

If the stable equilibrium was at the treatment threshold $N_{\min}$ or $N_{\max}$, then the dynamics of the two populations tended towards synchrony. From our limited investigation of parameter space, this was observed when connectivity between the populations was equal and greater than the internal growth rates of the populations (i.e., $r_{ij} = r_{ji} > r_{ii} = r_{jj}$; Table 2). Synchrony also occurred if the internal growth rates were unequal, but the total growth rates of the two populations were equal (i.e., $r_{uu} + r_{uv} = r_{vv} + r_{vu}$) and one population had a lower growth rate and higher connectivity to the other population. In this case, the population with higher connectivity became entrained by the dynamics of the "source" population.

A third type of behavior occurred when the total growth rates of the populations were not equal. In this case, the two populations oscillated with different periods. There was a discontinuity in the return map where u went from being treated once to twice (or two to three times, depending on the relative growth rates) before v was treated (Fig. 2c).

Table 2 Summary of parameter values under which different dynamics were observed

Internal growth rate	Connectivity	Behavior	Figure
$r_{uu} = r_{vv}$	$(r_{uv} = r_{vu}) \leq (r_{uu} = r_{vv})$	Phase locking	Fig. 2a
	$(r_{uv} = r_{vu}) > (r_{uu} = r_{vv})$	Synchrony	Figs. 2b and 4a
	$r_{uv} \neq r_{vu}$	Cycles	
$r_{uu} \neq r_{vv}$	$r_{uv} = r_{vu}$; incl. $r_{uv} = r_{vu} = 0$	Cycles	Fig. 2c
	$(r_{uu} + r_{uv}) = (r_{vu} + r_{vv})$	Synchrony or phase locking	Figs. 4b and S8
	Else	Phase locking or cycles	Fig. 2c
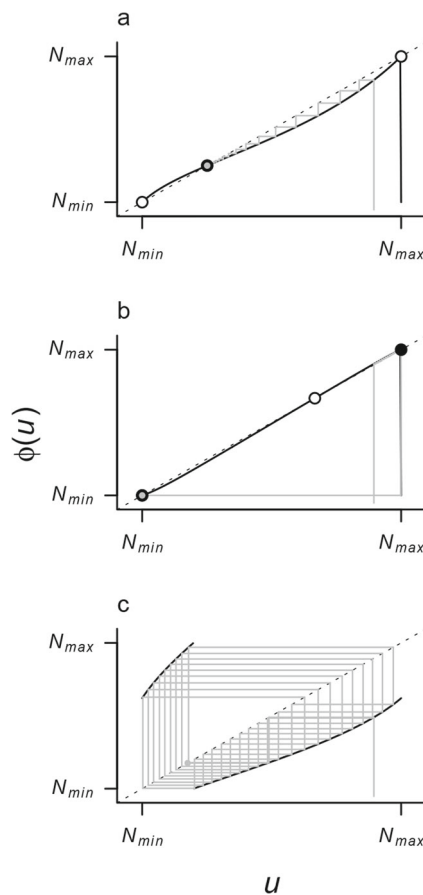
Fig. 2 Return maps for the population density u at re-treatment of v ($\phi(u^*)$) over increasing initial population density, u^*. **a** For low connectivity, there was a stable equilibrium in $(N_{\min}, N_{\max})$ (*black point*) and unstable equilibria at $N_{\min}$ and $N_{\max}$ (*white points*). **b** When connectivity was higher than internal growth, there was an unstable equilibrium in $(N_{\min}, N_{\max})$ and stable equilibria at $N_{\min}$ and $N_{\max}$, and the two populations synchronized. **c** For unequal connectivity, u was treated m or $m+1$ times before v was treated, yielding a discontinuity in the return map that resulted in cycles. The relative growth rates in each panel correspond to those in Fig. 1. The *gray lines* show 30 iterations of the return map (i.e., cobwebbing) from $u^* = 2.7$, ending at the *gray point*

This discontinuity resulted in periodic or seemingly chaotic behavior. Unlike in phase locking or synchrony, the population density u was not the same each time v was treated (Fig. 1c).

Parameter sensitivity

Increasing the connectivity between two patches resulted in changes to the long-term values of $\phi(u^*)$, the population density at re-treatment (Fig. 3 and Fig. S1). Some of these changes happened abruptly when the connectivity crossed a threshold (Fig. 3c, d), while others happened gradually (Fig. 3a). When the two populations had equal internal growth rates and equal connectivity, increasing the connectivity lead to increasing population density at re-treatment, until connectivity equalled the internal growth rates (scenario A in Table 1; Fig. 3a). At that point, the dynamics were phase-locked such that the population density at re-treatment was always the initial population density (i.e., $(\phi(u^*) = u^*) \; \forall \; u^*$; see Online Resource Figs. S2–S5 for illustrative animations).

When connectivity was increased from u to v only (e.g., scenario B in Table 1), the return map had a discontinuity because the total growth rate of v was higher than that of u. In that case, we observed periodic dynamics, the simplest being a two-point cycle that occurred near $r_{vu} = 0.8$ (Fig. 3b). In these two-point cycles, after the initial treatment of v, u will be treated once, then after the next treatment of v, u will be treated twice. This cycle repeats itself resulting in a pattern of treatments $v, u, v, u, u, v, u, v, u, u$, etc., with u having a lower population density at the treatment of v if u has been treated twice since the previous treatment of v.

When the internal growth rates of the populations were not equal (i.e., scenarios C and D in Table 1), the dynamics tended to be cyclic (Fig. 3c, d). However, abrupt changes from cyclic dynamics to stable points occurred as connectivity was increased to the point where the return map touched or crossed the 1:1 line. For example, in scenario D, when r_{vu} neared 0.51, the dynamics tended towards phase locking (Fig. S5). As connectivity increased from $r_{vu} = 0.35$ to $r_{vu} = 0.51$, the stable point approached $N_{\min}$ and the magnitude of the rescue effect decreased because u had a lower population density on treatment of v. When the total growth rates were exactly equal (i.e., $r_{vu} = 0.51$ such that $(r_{uu} + r_{uv}) = (r_{vu} + r_{vv})$), the two populations became synchronized (Fig. 3d; Table 2).

Increasing the connectivity between the patches did not necessarily result in a monotonic increase in the frequency of treatments (Fig. S6). For illustration, we focus on the frequency of treatments under scenario A, but with connectivity increasing to $r_{uv} = r_{vu} = 2.00$, and on scenario D with connectivity between $r_{vu} = 0.35$ and 0.52. In these scenarios, the internal growth rates were held constant (Table 1). Thus, we expected that the frequency of treatments would increase with increasing connectivity because the the total growth rate to the populations was increasing. However, we observed a sharp decline in the frequency of treatments in scenario A when connectivity exceeded the internal growth rate (Fig. 4a). In scenario D, the frequency of treatments declined over the region of phase locking (see Fig. 3d) as the stable point approached $N_{\min}$, reducing the impact of the rescue effect. The minimum frequency of treatments occurred where populations became synchronized at $r_{vu} + r_{vv} = r_{uv} + r_{uu}$ (i.e, $r_{vu} = 0.51$, Fig. 4b). In the Online Resource, we also considered a decline in the
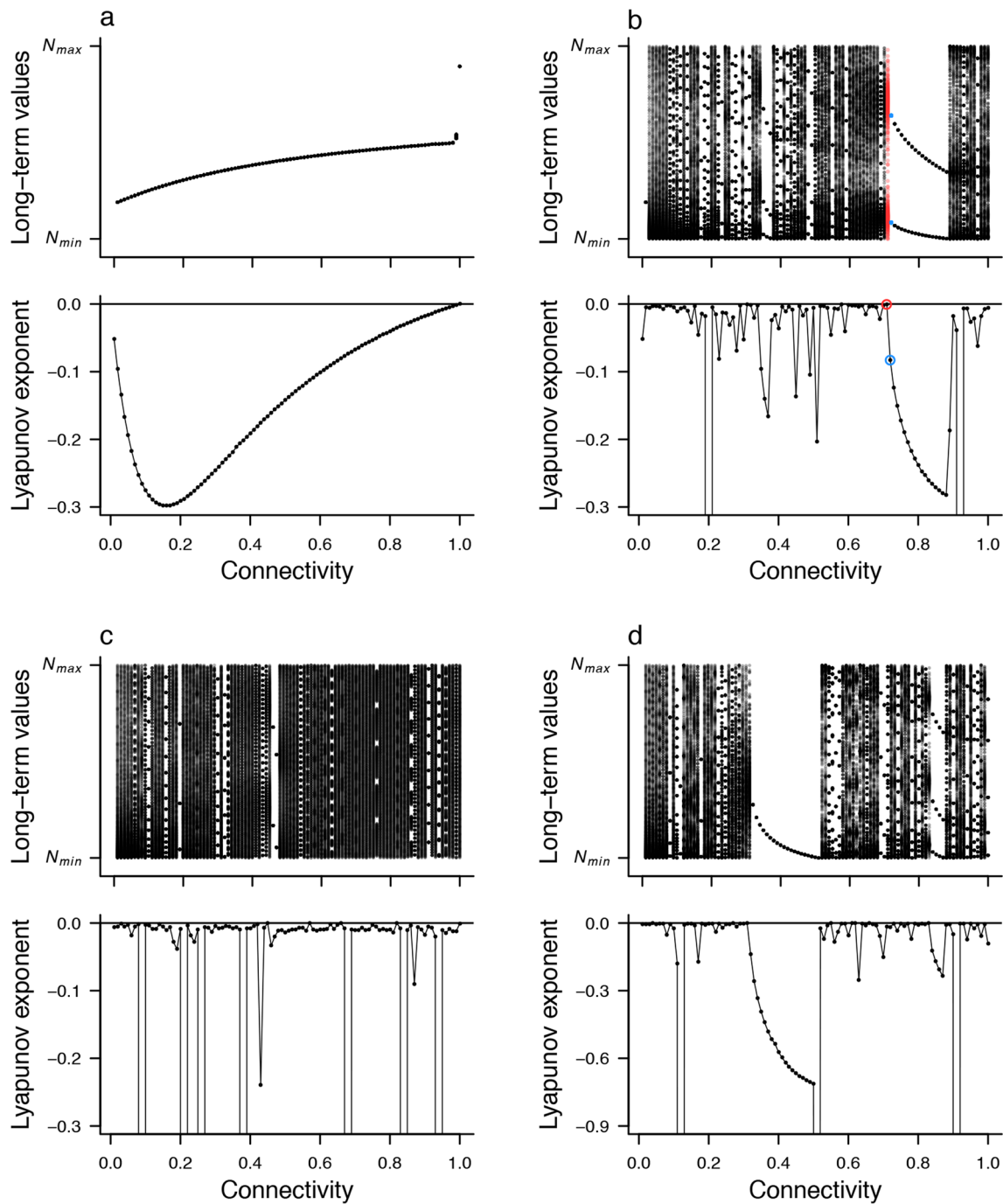
Fig. 3 Long-term values of $\phi(u^*)$ and the Lyapunov exponents λ under four different scenarios for changing connectivity (**a–d**; scenarios A–D in Table 1). In calculating long-term values, for each value of connectivity we plotted the last 500 of 2000 iterations starting at $u_0^* = 2.7$ (see Fig. S1 for results with other starting values). *Red and blue points* in (**c**) indicate the parameter values for stochastic simulations in Fig. 5. Online version in color

internal growth rate as connectivity increased such that $r_{ii} = 1 - r_{ij}$ and the total growth rates to populations remained constant in order to examine how connectivity affects the frequency of treatments independent of overall increases in

the growth rates. These simulations also showed a decrease in the frequency of treatments when populations became synchronized, and frequency of treatments remained low as connectivity increased further (Fig. S7).
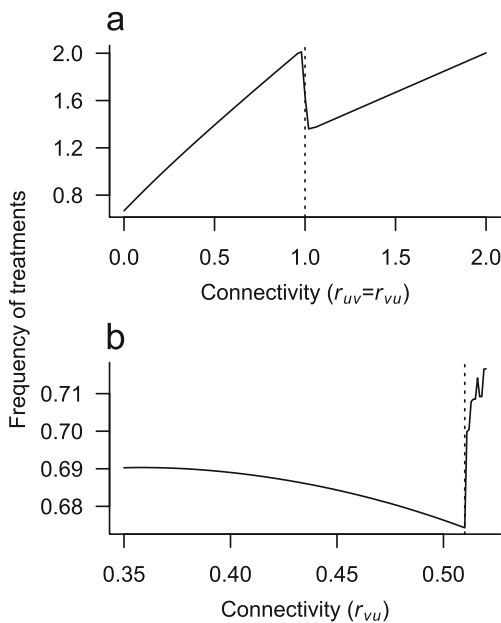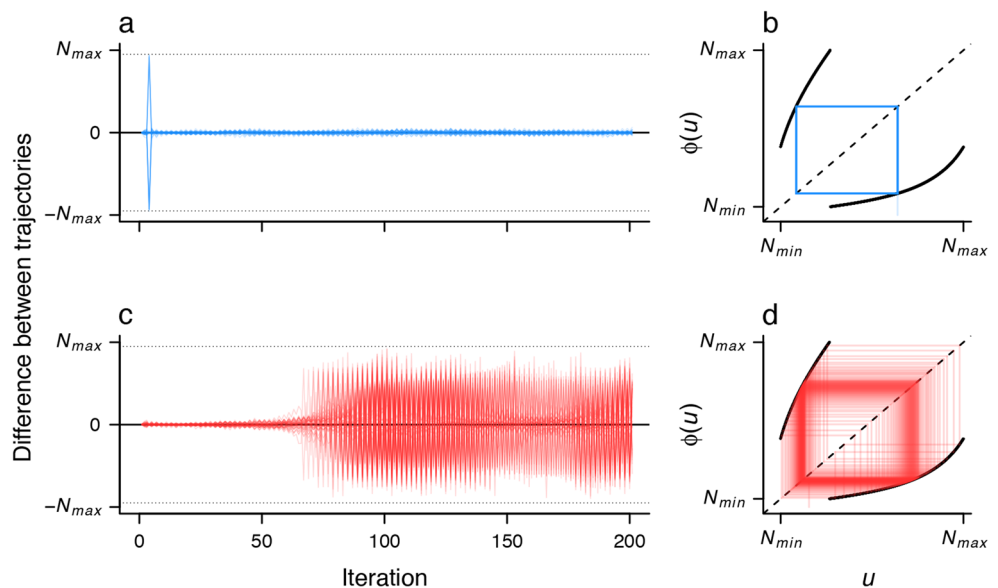
Fig. 4 The frequency of treatments over increasing connectivity. **a** In scenario A, the frequency of treatments drops when the connectivity exceeds internal growth rates (*dotted line*) and populations become synchronized (Table 2), but rises again as connectivity increases further due to increasing total growth rate. **b** In scenario D, the frequency of treatments declines over the region of phase locking (see Fig. 3d) as the stable point approaches N_{min}, reducing the impact of the rescue effect. The minimum frequency of treatments occurs where populations are synchronized at $r_{vu} + r_{vv} = r_{uv} + r_{uu}$ (i.e., $r_{vu} = 0.51$, *dotted line*; Table 2)

Testing for chaos

The time series of population density appeared chaotic when the period of the population cycles in the two patches was different (Fig. 1c). The bifurcation diagrams showed large regions of parameter space that had potentially chaotic dynamics (Figs. 1c and 3c–d). However, the Lyapunov exponent was not greater than zero in any of the scenarios (Fig. 3c–d), indicating the dynamics were not chaotic. Instead, the dynamics of two populations with different internal periods of oscillations appeared quasiperiodic. For periodic cycles, after iterating the return map a finite number of times, we returned to the exact value at which we started (e.g., Fig. 5b). Quasiperiodic cycles are differentiated from periodic cycles by cobwebbing the return map; over several treatments of v, $\phi(u^*)$ returned to the original branch of the return map very near to the starting point but not exactly at the starting point, such that the dynamics were shifted slightly (e.g., Fig. 5d). We note that a precise distinction between quasiperiodic and periodic dynamics is limited by the the number of times we could numerically iterate the return map.

Stochasticity

Small amounts of stochasticity added to the return map tended to shift quasiperiodic dynamics towards chaos such that two population initially close had very different population densities after 200 iterations. However, when the dynamics were periodic, the stochasticity was damped such that the fiducial trajectory and the perturbed trajectory remained relatively close over 200 iterations of the return map (Fig. 5a). A small change in r_{vu} from 0.72 to 0.71 in scenario C caused a transition from periodic to quasiperiodic dynamics (Fig. 5b, d). In the quasiperiodic case, the two trajectories drifted apart as the stochasticity accumulated (Fig. 5c). For scenario D, when r_{vu} was

Fig. 5 The effect of stochasticity differed with small changes in parameters. The difference between two trajectories initially separated by ϵ_0 remained small for parameters under which the deterministic model showed periodic dynamics (**a**), but increased for parameters under which the deterministic model showed quasiperiodic dynamics (**c**). The corresponding deterministic return maps of the fiducial trajectory for scenario B with $r_{vu} = 0.72$ (**b**) and $r_{vu} = 0.71$ (**d**) (see Fig. 3b). Online version in color

increased from 0.31 to 0.32, the deterministic dynamics went from quasiperiodic to phase locking (Fig. 3d). In this case, as in scenario C, stochasticity caused the trajectories to diverge for $r_{vu} = 0.31$ corresponding to the quasiperiodic dynamics, but stochasticity was damped when the deterministic dynamics exhibited phase locking (Fig. S9). This shows that small amounts of stochasticity can accumulate, when dynamics are not stable or periodic, and result in sensitivity to initial conditions that is characteristic of chaotic dynamics. Indeed, the Lyapunov exponents for the stochastic version of the model shown in Fig. 5 were $\lambda = 14.19$ (range 14.16 to 14.21) for $r_{vu} = 0.71$, compared to $\lambda = -0.001$ for the deterministic model. The Lyapunov exponent was also positive but smaller for the periodic dynamics corresponding to $r_{vu} = 0.72$, which showed damped oscillations (Fig. 5a).

Discussion

The current magnitude and extent of coupled human and natural systems is unprecedented and there is an urgent need to better understand the consequences of accelerating human impacts on natural ecosystems and the services that they provide (Millennium Ecosystem Assessment 2005). In this study, we considered the reciprocal interactions between the natural dynamics of parasite populations and human intervention in the form of parasite control. The resulting dynamics were surprisingly complex, and demonstrate the potential for unexpected behavior to result in policies that are well-meaning but have unintended and potentially perverse consequences for the health of ecosystems.

Implications for sea louse management

In Pacific Canada, salmon farms must treat with chemotherapeutants when sea louse populations exceed three motile sea lice per fish, a guideline that is meant to protect juvenile wild salmon from sea louse infestations during a vulnerable period of their migration (British Columbia Ministry of Agriculture and Lands 2005; Brooks 2009). However, our model showed that strict threshold control of parasites according to this policy may lead to asynchronous or even chaotic dynamics on adjacent farms connected by dispersal. In practice, whether dynamics are truly chaotic may not matter; given the timeframe of observations and management decisions, periodic dynamics may be just as challenging to predict and control. Increasing connectivity between populations tended to increase the frequency of treatments, unless populations were synchronized. Frequent, uncoordinated treatments are a problem because they

may hasten the evolution of sea louse resistance to current chemotherapeutants by allowing sea lice that are resistant to treatment to disperse and find mates on nearby, untreated farms (Aaen et al. 2015). Further, asynchronous parasite dynamics among farms make it difficult to ensure low parasite abundance during the wild juvenile salmon migration. Paradoxically, because threshold treatments tend to decouple parasite populations when not coordinated, this well-intended policy could mean high sea louse abundances on salmon farms along the migration route, transmission to juvenile salmon (Krkošek et al. 2006; Marty et al. 2010) and adverse impacts on wild salmon populations (Krkošek et al. 2011; Peacock et al. 2013).

The current treatment threshold policy does reduce louse abundance on farms, but more coordinated efforts to synchronize the parasite dynamics among farms may reduce reliance on chemotherapeutants. We found that at low levels of dispersal, the frequency of treatments increased with increasing connectivity, suggesting that dispersal among farms hinders control efforts. However, the frequency of treatments declined substantially when connectivity was high enough that parasite dynamics were synchronized between farms (Fig. 4a). In reality, dispersal of sea lice among farms is likely too low to synchronize parasite dynamics on adjacent farms by itself (Adams et al 2012; Foreman et al 2015), although shared environmental effects may help, see below). But for populations that were weakly coupled but had similar internal growth rates (e.g., have a similar number/age of hosts and are exposed to similar environmental conditions), synchrony could be induced by either treating populations at the same time (even if one population had not reached the threshold) or coordinating stocking and harvest among adjacent farms so that they start with the same initial conditions. Such strategies may reduce the potential for the rescue effect in louse populations on adjacent farms and therefore lower the frequency of treatments, but require coordinated effort among multiple stakeholders (e.g., different levels of government and industry). Pest management plans that require this kind of cooperation have been recommended (e.g., Brooks 2009; Peacock et al. 2013), but are still not implemented in many areas, including Pacific Canada.

Model limitations

Our simple model did not consider exogenous forces on the population dynamics such as variability in growth rates due to shared environmental conditions. Such forces are likely, due to the effect of temperature and salinity on settlement success (Bricknell et al. 2006), developmental rates (Groner et al. 2014; Stien et al. 2005), and survival (Johnson and Albright 1991a) of sea lice. Environmental conditions have

been proposed to result in synchrony of local population dynamics over wide geographic scales (i.e., Moran effects; Moran 1953). Indeed, such an effect has been shown in a variety of systems (e.g., Cheal et al. 2007; Grenfell et. al 1998). Sea louse populations on farmed salmon show annual cycles (Marty et al. 2010) that may be driven, in part, by changes in salinity and/or temperature (Johnson and Albright 1991b). The relative contributions of dispersal versus environment in driving synchrony of local populations is an ongoing question in ecology (Lande et al. 1999), and sea lice in networks of salmon farms may provide an ideal model system due to the extensive monitoring of louse populations and environmental conditions on salmon farms. These data have been used in statistical analyses aimed at management applications (e.g., Rogers et al. 2013; Revie et al. 2003) but could also be useful in answering questions of general interest in ecology.

Dynamics of coupled populations

There has been considerable theoretical interest in how dispersal affects the dynamics of coupled populations (e.g., Dey et al. 2014, 2015; Hastings et al. 1993; Kendall and Fox 1998; Goldwyn and Hastings 2011; Franco and Ruis-Herrera 2015). Our analysis expands on previous theoretical work in several ways. First, we considered control of populations when a threshold abundance was reached. Previous work has considered density dependence as part of the intrinsic dynamics of local populations (e.g., the Ricker model, Dey et al. 2015; Hastings et al. 1993), or periodic interventions such as feeding and harvest (e.g., Chau 2000). We consider a nonlinear reciprocal interaction between parasite populations and control intervention that had not yet been explored, although our approach shares similarities with work on Adaptive Limiter Control, discussed below (e.g., Sah et al. 2013). Second, we analyzed a continuous-time population model that may be more representative for some species, but were able to simplify our analysis by considering a discrete-time return map for the population density in one patch at the time of treatment in the other. This dynamical-systems approach has gained attention recently in the context of peak to peak dynamics (Rinaldi et al. 2001) and statistical methods for analyzing time series data (Sugihara et al. 2012), but also has broader applications for simplifying analyses of continuous-time models for interacting populations (Schaffer 1985). Finally, we varied both the internal growth rates and connectivities in our populations to explore scenarios where growth rates of the two populations differed and connectivity was not necessarily reciprocal. Many studies of coupled populations only consider equal connectivity (although see Dey et al. 2014; Franco and Ruis-Herrera 2015).

Increasing connectivity between two populations subject to control was expected to increase the frequency of treatments, but the simple model we developed displayed much more complex dynamics. Our results were consistent with other population models that show high connectivity leads to synchrony of populations while lower levels of connectivity lead to out-of-phase dynamics (Dey et al.2014, 2015). If the two populations had different periods due to unequal growth rates, the dynamics underwent periodic or quasiperiodic cycles. When dynamics were periodic, added stochasticity was damped such that the difference between nearby trajectories remained small. Hastings (1993) analyzed a coupled discrete logistic model and also found that the addition of stochasticity resulted in chaos for parameter values corresponding to a four-point cycle in the deterministic model, but stable population densities for parameter values corresponding to a two-point cycle in the deterministic model. This result highlights the fine line between predictable deterministic dynamics and chaos (Hastings 1993).

Previous work on threshold interventions in population dynamics have incorporated Adaptive Limiter Control (ALC; e.g., Sah et al. 2013). ALC involves a threshold intervention as in our model, but works to the opposite effect: where we consider control of a population when it goes above a threshold, ALC avoids population crashes by forcing immigration when the population drops below a threshold. Despite this difference, high thresholds for ALC tend to decouple subpopulations in a similar manner to our strict treatment threshold (Sah et al. 2013). This decoupling has opposite effects on fluctuations of the metapopulation depending on the migration rate between subpopulations. At high migration rates, subpopulations tend to be positively correlated, such that decoupling due to ALC is effective at increasing stability of the overall metapopulation. However, at low migration rates, subpopulations are more likely to be fluctuating out of phase and therefore ALC exacerbates this negative synchrony and decreases metapopulation stability. (Sah et al. 2013) found both theoretical and empirical evidence that these effects of ALC generally act to increase persistence of populations and metapopulations. Considering populations of pests and pathogens, persistence is not the desired outcome, providing an intriguing possibility that by decoupling populations, threshold effects may actually hinder eradication unless coordinated.

Conclusion

The complexity of coupled human and natural systems has gained attention as we recognize and attempt to understand our impact on natural ecosystems. For aquaculture, the interaction between farm management and natural pathogen

dynamics, including dispersal among farms, may lead to unpredictable dynamics that undermine our ability to maintain a healthy environment for both farmed and wild salmon. The successful management of disease in coastal ecosystems likely requires cooperation among different companies to synchronize and stabilize pathogen dynamics. This example emphasizes that human-natural couplings cross the boundaries of policy and governance, and cooperation among stakeholders at different levels is required to achieve the common goal of healthy and sustainable ecosystems that can support adaptive human populations.

Appendix A: Solution to ODE

The solutions to Eq. 1 are as follows:

$$
\begin{aligned}
u(t) &= f_u(t, u_0, v_0) \\
&= c_1 \exp\left[\frac{r_{uu} + r_{vv} + \alpha}{2} t\right] \\
&\quad + c_2 \exp\left[\frac{r_{uu} + r_{vv} - \alpha}{2} t\right]
\end{aligned}
\tag{A.1}
$$

$$
\begin{aligned}
v(t) &= f_v(t, u_0, v_0) \\
&= c_1 \left(\frac{r_{vv} - r_{uu} + \alpha}{2r_{uv}}\right) \exp\left[\frac{r_{uu} + r_{vv} + \alpha}{2} t\right] \\
&\quad + c_2 \left(\frac{r_{vv} - r_{uu} - \alpha}{2r_{uv}}\right) \exp\left[\frac{r_{uu} + r_{vv} - \alpha}{2} t\right],
\end{aligned}
\tag{A.2}
$$

where

$$
c_1 = \frac{2r_{uv}v_0 - u_0(r_{vv} - r_{uu} - \alpha)}{2\alpha}
\tag{A.3}
$$

$$
c_2 = \frac{u_0(\alpha + r_{vv} - r_{uu}) - 2r_{uv}v_0}{2\alpha}
\tag{A.4}
$$

$$
\alpha = \sqrt{(r_{uu} - r_{vv})^2 + 4r_{uv}r_{vu}}.
\tag{A.5}
$$

To get the time of the next treatment given the growth rates and initial conditions, we first rearrange Eqs. A.1–A.2. We denote the time of the next treatment of u and v as T_u

and T_v, respectively. The equations for T_u and T_v are the following:

$$
\begin{aligned}
2\alpha N_{\max} &= \exp\left(\frac{r_{uu} + r_{vv}}{2} T_u\right) \left[\left(\exp\left(\frac{\alpha}{2} T_u\right)\right.\right. \\
&\quad \left.- \exp\left(\frac{-\alpha}{2} T_u\right)\right) (2r_{uv}v_0 + u_0(r_{uu} - r_{vv})) \\
&\quad \left. + u_0\,\alpha \left(\exp\left(\frac{\alpha}{2} T_u\right) + \exp\left(\frac{-\alpha}{2} T_u\right)\right)\right]
\end{aligned}
\tag{A.6}
$$

$$
\begin{aligned}
4\alpha r_{uv} N_{\max} &= \exp\left(\frac{r_{uu} + r_{vv}}{2} T_v\right) \left[(2r_{uv}v_0\,(r_{vv} - r_{uu})\right. \\
&\quad + 4u_0\,r_{vu}r_{uv}\left(\exp\left(\frac{\alpha}{2} T_v\right) - \exp\left(\frac{-\alpha}{2} T_v\right)\right) \\
&\quad \left. + 2r_{uv}v_0\alpha\left(\exp\left(\frac{\alpha}{2} T_v\right) + \exp\left(\frac{-\alpha}{2} T_v\right)\right)\right].
\end{aligned}
\tag{A.7}
$$

In Eqs. A.6–A.7, T_u and T_v cannot be solved for explicitly, so we used a numerical root finding algorithm to determine T_u and T_v.

Appendix B: Development of return map

We used the dynamical system described in Eq. 2 to construct a return map that takes the population density u when v is treated and returns u the next time v is treated. We first consider the scenario where u is not treated in between consecutive treatments of v. We denote the time to the next treatment of v as T_{v0}. In this case, the resulting population density u at the next treatment of v is

$$
\phi(u^*) = f_u(T_{v0},\ u^*,\ N_{\min}),
\tag{B.1}
$$

where f_u is the solutions to Eq. 1, given in Appendix A. Next, we consider the case where u is treated once in between treatments of v. This leads to a return map of the form,

$$
\phi(u^*) = f_u(T_{v1},\ N_{\min},\ f_v(T_{u0}, u^*, N_{\min})),
\tag{B.2}
$$

where T_{u0} is the time from the initial treatment of v to the treatment of u and T_{v1} is the subsequent time from the

treatment of u to the next treatment of v. These two cases can be combined into a single equation as,

$$\phi(u^*) = \underbrace{H(\widetilde{T}_0)\, f_u\big(T_{v0},\ u^*,\ N_{\min}\big)}_{u \text{ not treated}}$$
$$+ \underbrace{H(\widetilde{T}_1)\,\big[1 - H(\widetilde{T}_0)\big]\, f_u\big(T_{v1},\ N_{\min},\ f_v(T_{u0}, u^*, N_{\min})\big)}_{u \text{ treated once}}.$$

(B.3)

We can continue in this way to get the equation that includes the possibility for u being treated twice in between treatments of v,

$$\phi(u^*) = \underbrace{H(\widetilde{T}_0)\, f_u\big(T_{v0},\ u^*,\ N_{\min}\big)}_{u \text{ not treated}}$$
$$+ \underbrace{H(\widetilde{T}_1)\,\big[1 - H(\widetilde{T}_0)\big]\, f_u\big(T_{v1},\ N_{\min},\ f_v(T_{u0}, u^*, N_{\min})\big)}_{u \text{ treated once}}$$
$$+ \underbrace{H(\widetilde{T}_2)\,[1 - H(\widetilde{T}_1)]\, f_u\big(T_{v2},\ N_{\min},\ f_v(T_{u1}, N_{\min}, f_v(T_{u0}, u^*, N_{\min}))\big)}_{u \text{ treated twice}}.$$

(B.4)

By induction, we arrive at the general equation for the return map, given in Eq. 3:

$$\phi(u^*) = \underbrace{\big[H(\widetilde{T}_0)\big]\, f_u\big(T_{v0},\ u^*,\ N_{\min}\big)}_{m=0}$$
$$+ \underbrace{\left[\sum_{m=1}^{\infty} H(\widetilde{T}_m) \prod_{n=0}^{m-1}[1 - H(\widetilde{T}_n)]\right] f_u\big(T_{vm},\ N_{\min},\ v_{m-1}\big)}_{m \geq 1}.$$

(B.5)

Appendix C: Algorithm describing return map

Because Eqs. A.6–A.7 cannot be solved for T_u and T_v, model analysis by the return map involved simulating successive treatments until v was treated next. The recursive algorithm we applied to calculate the population density u when v was treated next is the following:

```
function u_next(u, v, R)            Calculate the time to the next treatment of u
    evaluate T_u(u, v, R) = Tu      and the time to the next treatment of v
    evaluate T_v(u, v, R) = Tv
    if (T_u>T_v) then               If the time to treatment of v is less,
        return f_u(T_v, u, v)           return u when v is treated.
    else                            Otherwise, u is treated.
        v_new = f_v(T_u, u v)           Calculate v when u is treated and
        return u_next(Nmin, v_new, R)   repeat function with new initial values.
    end if
```

References

Aaen SM, Helgesen KO, Bakke MJ, Kaur K, Horsberg TE (2015) Drug resistance in sea lice: a threat to salmonid aquaculture. Trends Parasitol 31(2):72–81. doi:10.1016/j.pt.2014.12.006. http://linkinghub.elsevier.com/retrieve/pii/S1471492214002098

Abbott KC (2011) A dispersal-induced paradox: synchrony and stability in stochastic metapopulations. Ecol Lett 14(11):1158–1169. doi:10.1111/j.1461-0248.2011.01670.x

Adams T, Black K, Macintyre C, Macintyre I, Dean R (2012) Connectivity modelling and network analysis of sea lice infection in Loch Fyne, west coast of Scotland. Aquaculture Environ Interactions 3:51–63. doi:10.3354/aei00052. http://www.int-res.com/abstracts/aei/v3/n1/p51-63/

Aldrin M, Storvik B, Kristoffersen AB, Jansen PA (2013) Space-time modelling of the spread of salmon lice between and within Norwegian marine salmon farms. PLoS ONE 8(5):e64, 039. doi:10.1371/journal.pone.0064039

Becks L, Arndt H (2013) Different types of synchrony in chaotic and cyclic communities. Nat Commun 4:1359. doi:10.1038/ncomms2355. http://www.ncbi.nlm.nih.gov/pubmed/23322047

Birch L (1948) The intrinsic rate of natural increase of an insect population. J Anim Ecol 15–26. www.jstor.org/stable/1605

Bolker BM, Grenfell BT (1996) Impact of vaccination on the spatial correlation and persistence of measles dynamics. Proc Natl Acad Sci 93(22):12,648–12,653. http://www.pnas.org/content/93/22/12648.abstract

Bricknell IR, Dalesman SJ, O'Shea B, Pert CC, Luntz AJM (2006) Effect of environmental salinity on sea lice *Lepeophtheirus salmonis* settlement success. Dis Aquat Org 71(3):201–212. doi:10.3354/dao071201. http://www.int-res.com/abstracts/dao/v71/n3/p201-212/

British Columbia Ministry of Agriculture and Lands (2005) Fish Health Program 2003-2005. Tech. rep., Ministry of Agriculture and Lands, http://www.agf.gov.bc.ca/ahc/fish_health/Fish_Health_Report_2003-2005.pdf

Brooks KM (2009) Considerations in developing an integrated pest management programme for control of sea lice on farmed salmon in Pacific Canada. J Fish Dis 32(1):59–73. http://login.ezproxy.library.ualberta.ca/login?url=http://search.ebscohost.com/login.aspx?direct=true&db=eih&AN=36551408&site=ehost-live&scope=site

Brooks EN, Lebreton JD (2001) Optimizing removals to control a metapopulation: application to the yellow legged herring gull (*Larus cachinnans*). Ecol Model 136(2-3):269–284. doi:10.1016/S0304-3800(00)00430-0

Brown JHJ, Kodric-Brown A (1977) Turnover rates in insular biogeography: effect of immigration on extinction. Ecology 58(2):445–449. doi:10.2307/1935620. http://www.esajournals.org/doi/abs/10.2307/1935620

Chau NP (2000) Destabilising effect of periodic harvest on population dynamics. Ecol Model 127(1):1–9. doi:10.1016/S0304-3800(99)00190-8. http://www.sciencedirect.com/science/article/pii/S0304380099001908

Cheal AJ, Delean S, Sweatman H, Thompson AA (2007) Spatial synchrony in coral reef fish populations and the influence of climate. Ecology 88(1):158–69. doi:10.1890/0012-9658(2007)88[158:SSICRF]2.0.CO;2. http://www.ncbi.nlm.nih.gov/pubmed/17489464

Costello MJ (2009) How sea lice from salmon farms may cause wild salmonid declines in Europe and North America and be a threat to fishes elsewhere. Proc R Soc B Biol Sci 276(1672):3385–3394. doi:10.1098/rspb.2009.0771. http://rspb.royalsocietypublishing.org/content/276/1672/3385

Dey S, Goswami B, Joshi A (2014) Effects of symmetric and asymmetric dispersal on the dynamics of heterogeneous metapopulations: two-patch systems revisited. J Theor Biol 345:52–60. doi:10.1016/j.jtbi.2013.12.005

Dey S, Goswami B, Joshi A (2015) A possible mechanism for the attainment of out-of-phase periodic dynamics in two chaotic subpopulations coupled at low dispersal rate. J Theor Biol 367:100–110. doi:10.1016/j.jtbi.2014.11.028

Earn DJD, Rohani P, Grenfell BT (1998) Persistence, chaos and synchrony in ecology and epidemiology. Proc R Soc B Biol Sci 265(1390):7–10. http://rspb.royalsocietypublishing.org/content/265/1390/7.abstract

Earnshaw JC (1993) Lyapunov exponents for pedestrians. Am J Phys 61(5):401. doi:10.1119/1.17231. http://scitation.aip.org/content/aapt/journal/ajp/61/5/10.1119/1.17231

FAO (2014) The State of World Fisheries and Aquaculture 2014. Tech. rep., Food and Agriculture Organization of the United Nations, Rome. www.fao.org/publications

Foreman MGG, Chandler PC, Stucchi DJ, Garver KA, Guo M, Morrison J, Tuele D (2015) The ability of hydrodynamic models to inform decisions on the siting and management of aquaculture facilities in British Columbia. Canadian Science Advisory Secreteriat Research Document 2015/005:vii + 49, http://www.dfo-mpo.gc.ca/csas-sccs/

Franco D, Ruis-Herrera A (2015) To connect or not to connect isolated patches. J Theor Biol 370:72–80. doi:10.1016/j.jtbi.2015.01.029

Frazer LN, Morton A, Krkošek M (2012) Critical thresholds in sea lice epidemics: evidence, sensitivity and subcritical estimation. Proc R Soc B Biol Sci 279(1735):1950–1958. doi:10.1098/rspb.2011.2210. http://rspb.royalsocietypublishing.org/content/279/1735/1950

Fulford G, Roberts M, Heesterbeek J (2002) The metapopulation dynamics of an infectious disease: tuberculosis in possums. Theor Popul Biol 61(1):15–29. doi:10.1006/tpbi.2001.1553. http://linkinghub.elsevier.com/retrieve/pii/S0040580901915539

Galvanetto U (2000) Numerical computation of Lyapunov exponents in discontinuous maps implicitly defined. Comput Phys Commun 131(1):1–9. doi:10.1016/S0010-4655(00)00055-2. http://www.sciencedirect.com/science/article/pii/S0010465500000552

Goldwyn EE, Hastings A (2011) The roles of the Moran effect and dispersal in synchronizing oscillating populations. J Theor Biol 289(1):237–246. doi:10.1016/j.jtbi.2011.08.033

Grenfell BT, Wilson K, Finkenstadt BF, Coulson TN, Murray S, Albon SD, Pemberton JM, Clutton-Brock TH, Crawley MJ (1998) Noise and determinism in synchronized sheep dynamics. Nature 394(6694):674–677. doi:10.1038/29291

Groner ML, Gettinby G, Stormoen M, Revie CW, Cox R (2014) Modelling the impact of temperature-induced life history plasticity and mate limitation on the epidemic potential of a marine ectoparasite. PLoS ONE 9(2):e88,465. doi:10.1371/journal.pone.0088465

Hastings A (1993) Complex interactions between dispersal and dynamics: lessons from coupled logistic equations. Ecology 74(5):1362–1372. 10.2307/1940066

Hastings A, Powell T (1991) Chaos in a three species food chain. Ecology 72(3):896–903. http://www.jstor.org/stable/1940591

Hastings A, Hom CL, Ellner S, Turchin P, Godfray HCJ (1993) Chaos in ecology: is Mother Nature a strange attractor? Annu Rev Ecol Syst 24(1):1–33. doi:10.1146/annurev.es.24.110193.000245. http://www.jstor.org/discover/10.2307/2097171

Heggberget TG, Johnsen BO, Hindar K, Jonsson B, Hansen LP, Na Hvidsten, Jensen AJ (1993) Interactions between wild and cultured Atlantic salmon: a review of the Norwegian experience. Fish Res 18(1-2):123–146. doi:10.1016/0165-7836(93)90044-8

Hilborn R, Mangel M (1997) The ecological detective: confronting models with data, Monographs in Population Biology 28

Holt RD, McPeek MA (1996) Chaotic population dynamics favors the evolution of dispersal. Am Nat 148(4):709–718. doi:10.2307/2678832. http://www.jstor.org/stable/2556325

Igboeli OO, Burka JF, Fast MD (2014) *Lepeophtheirus salmonis*: a persisting challenge for salmon aquaculture. Anim Front 4(1):22–32. doi:10.2527/af.2014-0004. https://dl.sciencesocieties.org/publications/af/abstracts/4/1/22

Ives AR, Settle WH (1997) Metapopulation dynamics and pest control in agricultural systems. Am Nat 149(2):220–246

Jansen PA, Kristoffersen AB, Viljugrein H, Jimenez D, Aldrin M, Stien A (2012) Sea lice as a density-dependent constraint to salmonid farming. Proc R Soc B Biol Sci 279(1737):2330–2338. doi:10.1098/rspb.2012.0084. http://rspb.royalsocietypublishing.org/content/279/1737/2330.abstract

Johnson SC, Albright LJ (1991) Development, growth, and survival of *Lepeophtheirus salmonis* (Copepoda: Caligidae) Under

Laboratory Conditions. J Mar Biol Assoc U K 71(02):425–436. doi:10.1017/S0025315400051687

Johnson SC, Albright LJ (1991) The developmental stages of *Lepeophtheirus salmonis* (Krøyer, 1837) (Copepoda: Caligidae). Can J Zool 69(4):929–950. doi:10.1017/S0025315400051687

Keeling MJ, Gilligan CA (2000) Metapopulation dynamics of bubonic plague. Nature 407(6806):903–906. doi:10.1038/35038073

Kendall BE, Fox GA (1998) Spatial structure, environmental heterogeneity, and population dynamics: analysis of the coupled logistic map. Theor Popul Biol 54(1):11–37. doi:10.1006/tpbi.1998.1365

Kristoffersen AB, Rees EE, Stryhn H, Ibarra R, Campisto JL, Revie CW, St-Hilaire S (2013) Understanding sources of sea lice for salmon farms in Chile. Prev Vet Med 111(1-2):165–75. doi:10.1016/j.prevetmed.2013.03.015. http://www.ncbi.nlm.nih.gov/pubmed/23628338

Krkošek M, Lewis MA, Morton A, Frazer LN, Volpe JP (2006) Epizootics of wild fish induced by farm fish. Proc Natl Acad Sci 103(42):15506–15510. doi:10.1073/pnas.0603525103. http://www.pubmedcentral.nih.gov/articlerender.fcgi?artid=1591297&tool=pmcentrez&rendertype=abstract

Krkošek M, Bateman A, Proboszcz S, Orr C (2010) Dynamics of outbreak and control of salmon lice on two salmon farms in the Broughton Archipelago, British Columbia. Aquaculture Environ Interactions 1(2):137–146. doi:10.3354/aei00014. http://www.int-res.com/abstracts/aei/v1/n2/p137-146/

Krkošek M, Connors BM, Morton A, Lewis MA, Dill LM, Hilborn R (2011) Effects of parasites from salmon farms on productivity of wild salmon. Proc Natl Acad Sci 108(35):14,700–14,704. doi:10.1073/pnas.1101845108. http://www.pnas.org/content/108/35/14700

Lande R, Engen S, Sæther B (1999) Spatial scale of population synchrony: environmental correlation versus dispersal and density regulation. Am Nat 154(3):271–281. doi:10.1086/303240. http://www.jstor.org/stable/10.1086/303240

Lees F, Baillie M, Gettinby G, Revie CW (2008) The efficacy of emamectin benzoate against infestations of *Lepeophtheirus salmonis* on farmed Atlantic salmon (*Salmo salar* L) in Scotland, 2002–2006. PLoS ONE 3(2). http://journals.plos.org/plosone/article?id=10.1371/journal.pone.0001549

Levins R (1969) Some demographic and genetic consequences of environmental heterogeneity for biological control. Bull Ecol Soc Am 15(3):237–240. http://besa.oxfordjournals.org/content/15/3/237

Liebhold A, Koenig WD, Bjørnstad ON (2004) Spatial synchrony in population dynamics. Annu Rev Ecol Syst 35:467–490. doi:10.1146/annurev.ecolsys.34.011802.132516. http://www.annualreviews.org/doi/full/10.1146/annurev.ecolsys.34.011802.132516

Liu J, Dietz T, Carpenter SR, Alberti M, Folke C, Moran E, Pell AN, Deadman P, Kratz T, Lubchenco J, Ostrom E, Ouyang Z, Provencher W, Redman CL, Schneider SH, Taylor WW (2007) Complexity of coupled human and natural systems. Science 317(5844):1513. doi:10.1126/science.1144004. http://www.ncbi.nlm.nih.gov/pubmed/17872436

Marty GD, Saksida SM, Quinn TJ (2010) Relationship of farm salmon, sea lice, and wild salmon populations. Proc Natl Acad Sci 107(52):22,599–22,604. doi:10.1073/pnas.1009573108. http://www.pnas.org/content/107/52/22599.abstract

McCallum H, Harvell D, Dobson A (2003) Rates of spread of marine pathogens. Ecol Lett 6:1062–1067. doi:10.1046/j.1461-0248.2003.00545.x. onlinelibrary.wiley.com/doi/10.1046/j.1461-0248.2003.00545.x/pdf

Millennium Ecosystem Assessment (2005) Ecosystems and human well-being: synthesis, vol 5. Island Press, Washington, DC. http://www.who.int/entity/globalchange/ecosystems/ecosys.pdf; http://www.loc.gov/catdir/toc/ecip0512/2005013229.html. doi:10.1196/annals.1439.003

Moran P A P (1953) The statistical analysis of the Canadian Lynx cycle II. Synchronization and meteorology. Aust J Zool 1:291–298. doi:10.1071/ZO9530291. http://www.publish.csiro.au/?paper=ZO9530291

Oerke EC (2006) Crop losses to pests. J Agric Sci 144(01):31. doi:10.1017/S0021859605005708

Peacock SJ, Krkošek M, Proboszcz S, Orr C, Lewis MA (2013) Cessation of a salmon decline with control of parasites. Ecol Appl 23(3):606–620. doi:10.1890/12-0519.1. http://www.esajournals.org/doi/abs/10.1890/12-0519.1

Rae GH (2002) Sea louse control in Scotland, past and present. Pest Manag Sci 58(6):515–520. doi:10.1002/ps.491. http://onlinelibrary.wiley.com/doi/10.1002/ps.491/abstract

Ranta E, Kaitala V, Lindstrom J, Linden H (1995) Synchrony in population dynamics. Proc R Soc B Biol Sci 262(1364):113–118. doi:10.1098/rspb.1995.0184. http://rspb.royalsocietypublishing.org/content/262/1364/113.abstract

Revie CW, Gettinby G, Treasurer JW, Rae GH, Clark N (2002) Temporal, environmental and management factors influencing the epidemiological patterns of sea lice (*Lepeophtheirus salmonis*) infestations on farmed Atlantic salmon Salmo salar) in Scotland. Pest Manag Sci 58(6):576–584. http://onlinelibrary.wiley.com/doi/10.1002/ps.476/abstract

Revie CW, Gettinby G, Treasurer JW, Wallace C (2003) Identifying epidemiological factors affecting sea lice *Lepeophtheirus salmonis* abundance on Scottish salmon farms using general linear models. Dis Aquat Org 57(1-2):85–95. http://www.int-res.com/abstracts/dao/v57/n1-2/p85-95/

Rinaldi S, Candaten M, Casagrandi R (2001) Evidence of peak to peak dynamics in ecology. Ecol Lett 4:610–617. http://onlinelibrary.wiley.com/doi/10.1046/j.1461-0248.2001.00273.x/full

Rogers LA, Peacock SJ, McKenzie P, DeDominicis S, Jones SRM, Chandler P, Foreman MGG, Revie CW, Krkošek M (2013) Modeling parasite dynamics on farmed salmon for precautionary conservation management of wild salmon. PLoS ONE 8(4):e60,096. doi:10.1371/journal.pone.0060096

Sah P, Paul Salve J, Dey S (2013) Stabilizing biological populations and metapopulations through Adaptive Limiter Control. J Theor Biol 320:113–23. doi:10.1016/j.jtbi.2012.12.014. http://www.sciencedirect.com/science/article/pii/S002251931200642X

Samways MJ (1979) Immigration, population growth and mortality of insects and mites on cassava in Brazil. Bull Entomol Res 69(03):491–505. doi:10.1017/S000748530001899X

Schaffer WM (1985) Order and chaos in ecological systems. Ecology 66(1):93–106. http://www.esajournals.org/doi/abs/10.2307/1941309

Silva A (2003) Morphometric variation among sardine (*Sardina pilchardus*) populations from the northeastern Atlantic and the western Mediterranean. ICES J Mar Sci 3139(03):1352–1360. doi:10.1016/S1054. http://icesjms.oxfordjournals.org/content/60/6/1352.short

Sprott J (2003) Chaos and time-series analysis. Oxford University Press, http://sprott.physics.wisc.edu/chaostsa/

Steen H, Ims RA, Sonerud GA, Steen H (1996) Spatial and temporal patterns of small-rodent population dynamics at a regional scale. Ecology 77(8):2365–2372. http://www.esajournals.org/doi/abs/10.2307/2265738

Stien A, PA Bjørn, Heuch PA, Elston DA (2005) Population dynamics of salmon lice *Lepeophtheirus salmonis* on Atlantic salmon and sea trout. Mar Ecol Prog Ser 290:263–275. doi:10.3354/meps290263

Sugihara G, May R, Ye H, Hsieh Ch, Deyle E, Fogarty M, Munch S (2012) Detecting causality in complex ecosystems. Science 338(6106):496–500. doi:10.1126/science.1227079. http://www.ncbi.nlm.nih.gov/pubmed/22997134 http://www.sciencemag.org/content/338/6106/496.abstract

Tompkins DM, Carver S, Jones ME, Krkošek M, Skerratt LF (2015) Emerging infectious diseases of wildlife: a critical perspective. Trends Parasitol 31(4):149–159. doi:10.1016/j.pt.2015.01.007. http://linkinghub.elsevier.com/retrieve/pii/S1471492215000197

Van Bael S, Pruett-Jones S (1996) Exponential population growth of monk parakeets in the United States. The Wilson Bull 108(3):584–588. http://www.jstor.org/stable/4163726

Walker PJ, Winton JR (2010) Emerging viral diseases of fish and shrimp. Vet Res 41(6). doi:10.1051/vetres/2010022